Journal of Engineering and Applied Sciences 13 (Special Issue 3): 3169-3176, 2018
ISSN: 1816-949X

Use of ICT's to Generate Real-Time Alerts Based on the Automatic Analysis by the Artificial Vision System that Monitors Eruptive Processes

Cruz Christyan, Viteri Francisco, Barrera Kevin and Dario Jose Mendoza Chipantasi
Departamento de Ciencias de la Energia y Mecanica, Universidad de las Fuerzas Armadas ESPE,
171-5-231B Sangolqui, Ecuador

Abstract: The great potential, reliability and the high number of applications made through artificial vision, are fundamental for the development of a monitoring system pyroclastic flows for active volcanoes axis through a platform called Raspberry Pi based on free software (Ubuntu), the great potential of it allows you to run several software for the application of computer vision techniques, make data processing and also control outputs from the same board. Thus, the main points to note when using an embedded system are a stable data acquisition, fast processing and control outputs to operate alarm systems but especially, the cost is reduced and reliable system.

Key words: Alarms, pyroclastic flows, Raspberry Pi, artificial vision, reliable system, control

INTRODUCTION

The use ICTs to develop and deploy new applications that generate large-scale utility in risk areas, provides a great social contribution in the event of a natural disaster of volcanic character. Today technology has advanced at great scale, reducing costs and sizes in processors and placing them on the market for commercialize them as in the case of platforms such as Raspberry Pi whose functionality embedded system is the main aspect that can be highlighted as allows data acquisition, processing and generating signals (Duck *et al.,* 2015; Guin *et al*., 2014) through its ports which combined with free programming language as the case of Python allows the realization of applications focused on monitoring eruptive processes through the use of artificial vision and generation of early warnings.

Alarm systems actived in case of eruption may be sound and light type where the use of GPIO ports (Inputs and Outputs General Purpose), provide connections from the control board to the external environment, before processing performed (Duck *et al*., 2015). Within audible alarms the best example and implemented are sirens due to its large earshot to alert the population which together with system lights of high brightness can form a preventive system of high efficiency that should be placed in strategic points within the city. Moreover, easy access to navigate through the Internet, either from a desktop PC, laptop or a smartphone, provides first hand through an application, the status of the different variables that they can be monitored on a volcano such as the status of its activity, amount and direction of pyroclastic flows.

MATERIALS AND METHODS

Artificial vision applied to the detection of lava and surfaces: The main objective of digital image processing is find information within a matrix of pixels (Sakaguchi *et al*., 2012; Nie *et al*., 2013) in this case is the pursuit of lava and pyroclastic flows within a sequence of images (video), captured through a sensor (camera). The software used for digital processing stage is Python, because of its features like: speed, simplicity, order and especially, most of the libraries needed to compile already are included, the other libraries must be installed from the terminal to command through.

Images acquisition : The images are captured by a camera attached to one of the USB ports (Fig. 1), individually, sequentially or video (Nie *et al*., 2013; Soltani *et al*., 2015). This camera is connected to a servomotor which provides rotation in the visible range of the crater and in the case of an eruption, keeps tracking of pyroclastic flows.

Next stage is image digitalization where catches become arrays of rows and columns with values for each pixel. Reading through programming it is done with the

Corresponding Author: Cruz Christyan, Departamento de Ciencias de la Energia y Mecanica,
Universidad de las Fuerzas Armadas ESPE, 171-5-231B Sangolqui, Ecuador

(a)

(b)

Fig. 1: a) Snowy volcano Tungurahua and b) In eruptive process

command 1. Where cap is a storage array for images read by the camera 0. Command 1 video acquisition:

Cap = cv2. Video Capture (0)

Image processing and detection of variables: After capturing the image, this is in the RGB color space (Red, Green and Blue) but for processing must be passed to HSV (Hue, Saturation and Value), command 2 because it facilitates the recognition of palettes specific between minimum and maximum values (Nie *et al*., 2013; Soltani *et al*., 2015) in addition to separating the layer brightness. Command 2 conversion from RGB to HSV parameters:

Hsv = cv2. cvt Color (frame, cv2. COLOR_BRG2HSV)

Applying layers of erosion and dilation with command 3, to improve the morphology and better define the contours of an image. These things must be applied at least two or three times to get a better definition of the edges of an image. Command 3 Application of layers of erosion and dilation:

- Im = cv2. erode (im, cv2. getStructureingElement)
- Im = cv2. dilate (im, cv2. getStructureingElement)

To improve the image is necessary a Trackbar (Command 4) to modify the maximum and minimum HSV parameters (Erkent and Bozma, 2012; Mahapatra *et al*., 2015) those values will be used to create a mask (Command 5) which will function as a filter allowing passage only nuances in a set range, this range will consist of shades of lava and pyroclastic flows. Finally through another window the result of the binarized image (Command 6) is displayed and in white color is indicated the area to be the variable to be measured (Paolillo *et al*., 2016; Mahapatra *et al*., 2015) and also indicate the presence of lava or pyroclastic flows (Fig. 18).

Command 4 creation of trackbar:

- Cv2. create trackbar ('Hmax', 'Config', 0, 256)
- Cv2. create trackbar ('Hmin', 'Config', 0, 256)
- Cv2. create trackbar ('Smax', 'Config', 0, 256)
- Cv2. create trackbar ('Smin', 'Config', 0, 256)
- Cv2. create trackbar ('Vmax', 'Config', 0, 256)
- Cv2. create trackbar ('Vmin', 'Config', 0 ,256)

Command 5 mask with max and min HSV values:

- Im = cv2.in Range (hsv, np. array ((Hmin, Smin, Vmin)) np. array ((Hmax, Vmax, Smax)))

Command 6 show the binarized image:

- Cv2.im show ('in Range', im)

The state of eruption of the volcano will be considered active when in the binarized image exists a white area of over 500 pixels (Command 7) which would evidence detection pyroclastic flows or lava (Mahapatra *et al*., 2015).

Command 7 detection of the area of interest inside 'im':

- M = cv2. moments (im)
- If M ['m00']>10000

Alarm and communication systems: One of the key parts for early warning to the surrounding communities of a volcano and to prevent risks that could cause an eruption (Borla *et al*., 2015) are visual alarms placed in strategic locations and areas of high visibility for communities and high-risk sectors.

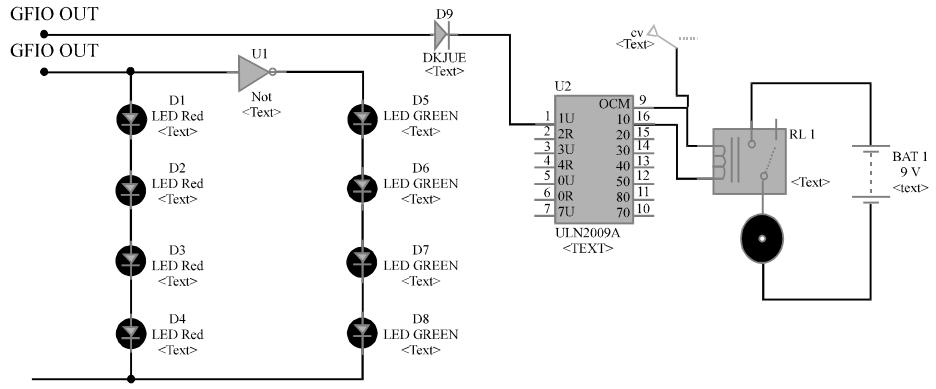

Fig. 2: Electrical connection scheme

For sequential operation of eruption process detection and alarm activation, after detection of an area of interest in 'im' is necessary program GPIO ports and configure them as outputs. Command 8 configuration of GPIO ports as output:

- GPIO.setup (15, GPIO. OUT)
- GPIO.setup (16, GPIO. OUT)

Control ports are operated by programation through the following command. Command 9 for control of GPIO ports:

- GPIO.output (15, True) # on
- GPIO.output (16, False) # off

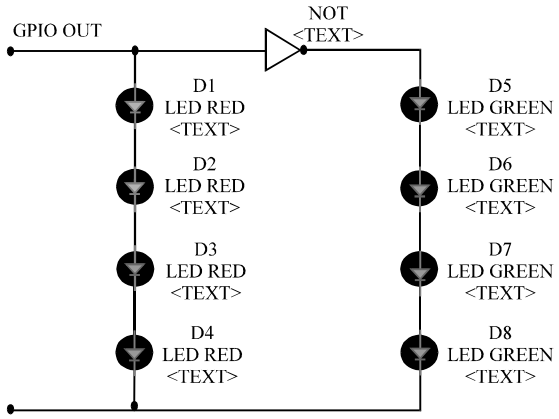

Fig. 3: LED connection diagram

Visual alarms: They are observed directly as LED lights or in a massive case the GPIO port could be connected to a potency system through a relay (Fig. 2) whose electrical diagram is detailed in the following scheme.

Lighting system: The first part of the circuit Fig. 3, are the LED visual alarms, same as have two states, on-off, whose colors are red and green, respectively, indicating states of security and rash. For control is necessary only one GPIO port configured as a digital output in order to avoid using multiple ports, turning slow processing when sending signals to the pins. In that place and to optimize resources and ports is imperative improved electronic design through the use of logic gates (Guin and Tehranipoor, 2014; Copetti *et al*., 2016) which only invert the signal, achieving the desired outputs through a single pin.

Application for smartphone and pc: The creation of the channel for subscription must be made in the "http://www.pushetta.com/" page where the creation of an account is required and then add a channel and insert an image for identification, give properties that is public and a message to display (Fig. 4).

First of all to receive real-time notification alert monitored volcano eruption, you need to download a free app from the Play Store for Android and iOS App Store, called "Pushetta". Then is necessary a subscription to the monitoring previously created channel called "Volcanes_ESPE001" (Fig. 5).

In addition, monitoring can be performed directly from the website "http://www.pushetta.com/", performing the same subscription. The result is a real-time alert status of the volcano active if the eruptive process existed (Fig. 12).

Sound alarm: A port is configured as a digital output, to a 2N222 transistor whose configuration is common emitter (Copetti *et al*., 2016; Kim *et al*., 2015), it serves to amplify the output current and simultaneously works as a switch when entering the zone of saturation, allowing the closure of the circuit and relay activation. The current emitted by

Fig. 4: Creating the channel in the Pushetta page

Fig. 5: Capture, channel subscription

a GPIO port is 16 mA which is insufficient to directly activate a 5V DC motor or turn a relay on. To determine if the transistor enters the saturation zone is necessary to calculate the base current l_R which should be greater than the relationship between the collector current I_C and gain β of the transistor 2N2222:

$$I_B > \frac{I_C}{\beta} \quad (1)$$

Where:

$$I_B = \frac{V_{CC}\text{-}0.7\ V}{R1} \quad (2)$$

$$I_B = \frac{5\text{-}0.7\ V}{2.2\ K},\ I_B = 1.95\,[mA]$$
$$I_C = \frac{V_{DD}}{R2},\ I_C = \frac{SV}{100},\ I_C = 0.05\,[A] \quad (3)$$

Analyzing the relationship:

$$I_B > \frac{IC}{\beta}$$
$$1.95mA > \frac{0.05\ A}{150}$$
$$1.95 > 0.33\ mA$$

Concluding that the values of resistors Fig. 6 (R1, 2.2 Ω and R2, 100 Ω) and the transistor 2N2222 when applying a pulse up through the control pin, the

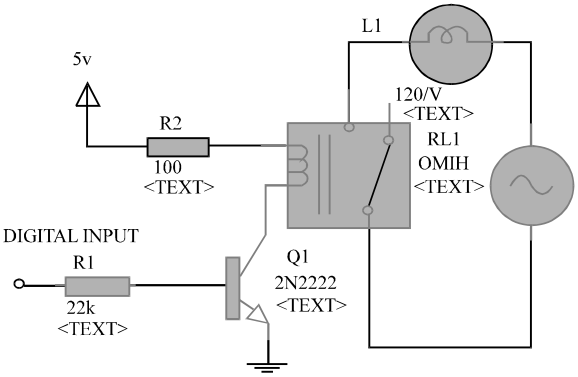

Fig. 6: Current gain scheme and uncoupling of the control part and power

transistor will enter the saturation zone (Guin *et al*., 2014; Kim *et al*., 2015) activating the relay and the power stage.

Comunication systems: The types of communication that can be used for data transmission, applicable to the project are: Bluetooth, Ethernet (html) through Wi-Fi, LAN, 3GSM and 4G LTE networks allowing interaction with the external environment (Lloret *et al*., 2013) for monitoring eruptive process if there are.

The main advantages of using a html communication on the Bluetooth is the global reach it generates to send data to a server which can be accessed world. To solve the problem of hich in remote areas hardly be bile networks such as LTE 4G or accessed through modems mobile y because they have extensive ote access and provide internet access (Lloret *et al*., 2013; Gutierrez, 2011), depending on the area, there will be more or less coverage and that will depend on access to 4G LTE or 3GSM network. Where the main advantage of 4G over 3G network is the speed of data transfer that is approximately 80 and 7.2 Mbps for each network, respectively (Soltani *et al*., 2015).

Volcanes-ESPE001
Actividad de volcanes en Ecuador!!

We could get access to internet from a modem, whose coverage extends to all parts of the area where network coverage is found in case of areas surrounding volcanoes coverage has a range of about 80 km, enough distance to keep informed the residents. Other hand the use of a LAN connection has speed data transmission of 10 Mbps but has a limit on coverage ranging from 200 m and a maximum of 1 km (Zhang *et al*., 2010). Being insufficient to cover a whole population.

RESUTLS AND DISCUSSION

Experimental results

Images acquisition and processing: For processing images can be acquired sequentially through a video camera (Fig. 7) or individually through a file format jpg or png (Fig. 8).

Mask created with the maximum and minimum values of trackbar (Fig. 9), allows the passage of only the colors set in the range of color shades. This is shown in Fig. 10, the result of processing applied to Fig. 8. Where you can see a volcano in eruption process emitting pyroclastic flows and volcanic lava.

Fig. 7: Video capture

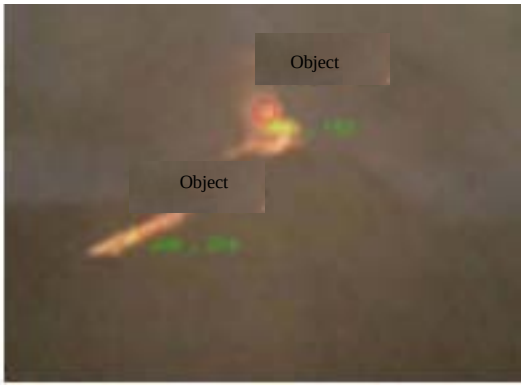

Fig. 8: Image format jpg

After detection blank area of over 500 pixels (considered as rash), alarm systems are activated (Fig. 11), red LEDs indicate status active volcano and Fig. 12 notification sent.

The efficiency of the alarm system is 92% (Fig. 13), this result was gotten based on random tests taken at intervals of 1 h in continuous operation of the system. And the optimal times for turn on the light system is 0.5 sec and to get notifications is 12 sec (Lloret *et al*., 2013; Zhang *et al*., 2011).

Servomotor control for monitoring: Controlling the servomotor based on tracking the center of the detected area, thus, a control on the x axis is set, for this it is necessary to compensate the error obtained through Eq. 5. The control pulses (Fig. 15) ranging from 0-12.5, scaling with respect to the range of 0-270° rotated by the

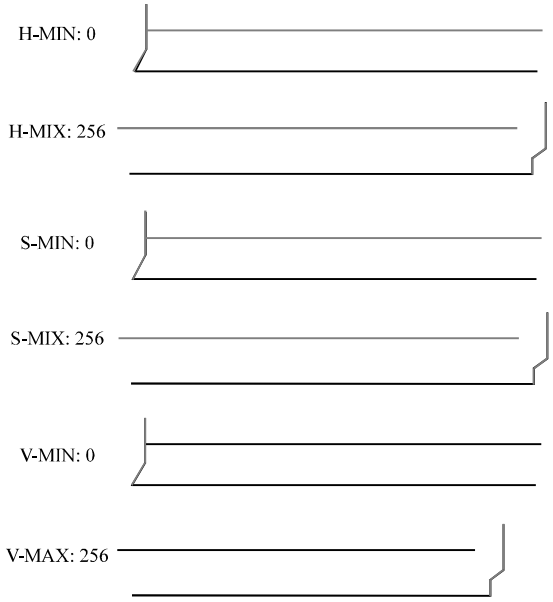

Fig. 9: Trackbar

Fig. 10: Processed image

Fig. 11: Indicative leds

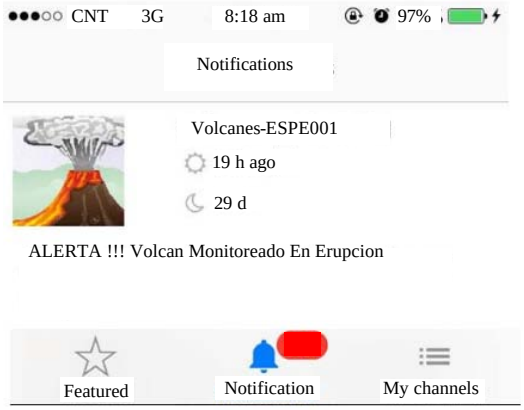

Fig. 12: Notification received on iOS

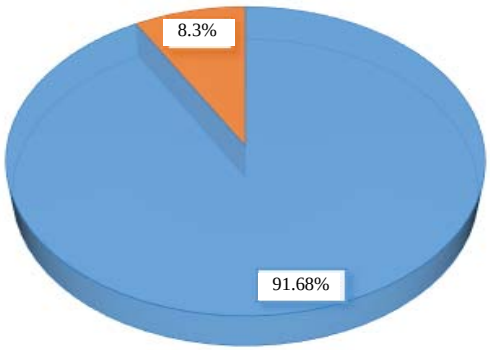

Fig. 13: Percentage efficiency of the system based on Table 1

servomotor is directly proportional where 30° is the angle of view covering a compact camera corresponds a value of 1.3 pulses.

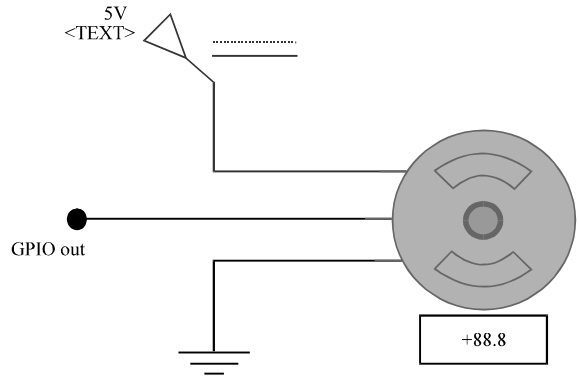

Fig. 14: Servomotor control, electronic conection

Table 1: Testing time delays to trigger alarms

Tests/effective time	Time-turn on lights (0.5 sec)	Time-get notification (12 sec)	System efficiency (100%)
1	0.601	12.3	96.80
2	0.700	12.6	93.90
3	0.721	14.1	84.40
4	0.650	12.5	95.05
5	0.553	12.9	92.93
6	0.768	13.3	88.90
7	0.750	12.9	92.04
8	0.767	13.5	87.60
9	0.733	12.8	92.20
10	0.690	12.6	93.00

In order to obtain a mathematical model that dictaminate the error is established a proportionality between the pulses to send and the central position of the object detected measured in pixels within the window. Where 600 is the maximum number of pixels within the window and 1.3 is the maximum pulse to be sent.

The equation is obtained through the linear model of Eq. 4 and the experimental data in Table 2. Where m is the slope obtained from Eq. 6, the points (x1, y1) conresponden value (600, 1.3) (Fig. 15):

$$y-y1 = m(x-x1)$$
$$y-1,3 = 0.0021(x-600) \quad (4)$$

$$y = 1.3+0.0021x-1.3$$
$$y = 0.0021x \quad (5)$$

$$m = \frac{y2-y1}{x2-x1}$$
$$m = \frac{1.3-0}{600-0} \quad (6)$$
$$m = 0.0021$$

The result of the Eq. 5. Will be stored in a variable called "pu" which is what made the compensation, adding

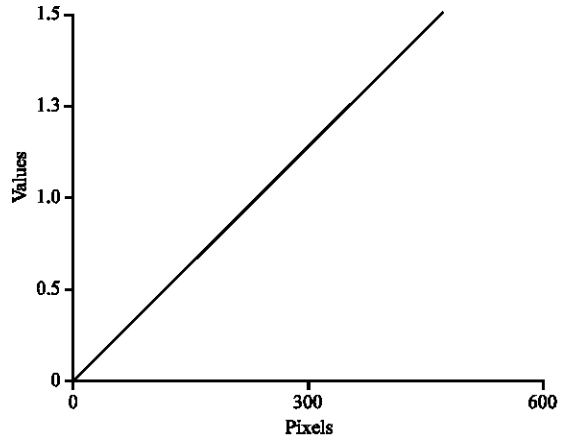

Fig. 15: Pixels in window (x-axis horizonal) vs pulses to control the servomotor (y-axis vertical)

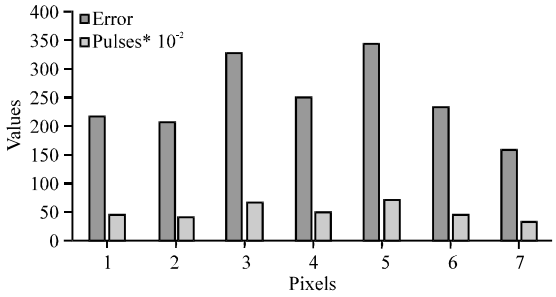

Fig. 16: Pulse compensation based on errors obtained

Table 2: Error offset and pulses as tested

Error	Pulses*$10^{(-2)}$
220	46.20
210	44.10
330	69.30
250	52.50
344	72.24
232	48.72
160	33.60

or subtracting a variable called "sol", this will send the number of resulting pulses to the port GPIO (command 10). Command 10 compensation and sending pulses-port:

- If (error >200)
- Sol = sol-pul
- P. Change Duty Cycle (sol)
- Else
- Sol = sol+pul
- P. Change Duty Cycle (sol)

CONCLUSION

The centralization of the main plane of an eruption, that is the approach to the place of the volcano where there is greater amount of pyroclastic flows and volcanic lava is an important aspect to have information about the direction in which these are to be moved. For monitoring made towards the center of the detected objects, compensation is employed by pulses sent to the anchored servomotor to a camera, using Eq. 5 and Table 2 that dictate compensation pulse based on the obtained error displacement of the center screen relative to the center of the detected elements.

The warning systems such as light alarms, sirens, messages on mobile applications which are transmitted in real time to vulnerable populations time, they can be vital to forewarn and especially, save lives because of the short time that used to be activated in the case of lights and sirens of 500 msec, the drive is immediate because of the electronic control through which are actuated. While notifications takes about 12 sec with an error of plus or minus 2 sec, to arrive, using internet with 2.5 Mbps speed for the sender and the receiver. Showing that the system based on the tests performed has an efficiency of 90.03% which can be enhanced if a better internet connection is used as fiber optics.

Free software used to perform the monitoring program (Python) was chosen for its low computational cost for processing and because it allows control of the GPIO ports. The program acquires images in RGB and processes them as matrices such processing is to move the image to HSV, then apply several layers of erosion and dilation to improve, then through parameter setting HSV noise is eliminated which is generated by disturbances and camera sensor and choose only one winning specific shades of color known as "layer" which has the color gamut of volcanic lava and pyroclastic flows emitted by the volcano, the layers between HSV values are (H min = 0, S min = 158 min = 108 V) and (H_{max} = 256, S_{max} = 188, V_{max} = 256). Leaving only blank area of interest which the area is calculated and is considered significant if it is >1000 pixels, because of the scaling 1-10000 for the mirror screen.

ACKNOWLEDGEMENTS

Sincerely grateful to the Universidad de las Fuerzas Armadas ESPE-Latacunga, especially, to the engineer Dario Mendoza. To my mom, family and ceris. Thanks.

REFERENCES

Borla, O., G. Lacidogna and A. Carpinteri, 2015. Piezonuclear Neutron Emissions from Earthquakes and Volcanic Eruptions. In: Acoustic, Electromagnetic, Neutron Emissions from Fracture and Earthquakes, Carpinteri, A., L. Giuseppe and M. Amedeo (Eds.). Springer, Berlin, Germany, ISBN:978-3-319-16954-5, pp: 135-151.

Copetti, T., G.C. Medeiros, L.B. Poehls and F. Vargas, 2016. NBTI-Aware design of integrated circuits: A hardware-based approach for increasing circuits life time. J. Electron. Test., 32: 315-328.

Duck, M., M. Schloesser, V.S. Waasen and M. Schiek, 2015. Ethernet based time synchronization for Raspberry Pi network improving network model verification for distributed active turbulent flow control. Control Theor. Technol., 13: 204-210.

Erkent, O. ans I.H. Bozma, 2012. Artificial potential functions based camera movements and visual behaviors in attentive robots. Auton. Robots, 32: 15-34.

Guin, U., D.D. Mase and M. Tehranipoor, 2014. Counterfeit integrated circuits: Detection, avoidance and the challenges ahead. J. Electron. Test., 30: 9-23.

Gutierrez, P.A.A., 2011. A simplified internet routing architecture. Mobile Networks Appl., 16: 433-445.

Kim, S.Y., N.X. Hieu and J.W. Lee, 2015. A broad-band V-band power amplifier using a reduced access-resistance transistor layout in 65-nm CMOS. Analog Integr. Circuits Signal Process., 82: 487-493.

Lloret, J., K.Z. Ghafoor, D.B. Rawat and F. Xia, 2013. Advances on network protocols and algorithms for vehicular ad hoc networks. Mob. Netw. Appl., 18: 749-754.

Mahapatra, P.K., S. Sethi and A. Kumar, 2015. Comparison of artificial immune system and particle swarm optimization techniques for error optimization of machine vision based tool movements. J. Inst. Eng. (India) Ser. C., 96: 363-372.

Nie, F., Y. Wang, M. Pan, G. Peng and P. Zhang, 2013. Two-dimensional extension of variance-based thresholding for image segmentation. Multidimension. Syst. Signal Process., 24: 485-501.

Paolillo, A., A. Faragasso, G. Oriolo and M. Vendittelli, 2016. Vision-based maze navigation for humanoid robots. Auton. Robots, 41: 293-309.

Sakaguchi, H., M. Kamei, K. Nishida, Y. Terasawa and T. Fujikado *et al*., 2012. Implantation of a newly developed direct optic nerve electrode device for artificial vision in rabbits. J. Artif. Organs, 15: 295-300.

Soltani, M., M. Omid and R. Alimardani, 2015. Egg volume prediction using machine vision technique based on pappus theorem and artificial neural network. J. Food Sci. Technol., 52: 3065-3071.

Zhang, Y., C. Wang, H.H. Chen and M. Daneshmand, 2011. Editorial for WICON, 2010 on recent advances in wireless internet. Mobile Networks Appl., 16: 745-747.